ADAPTIVE ISOGEOMETRIC METHODS WITH HIERARCHICAL SPLINES: AN OVERVIEW

Cesare Bracco

Dipartimento di Matematica e Informatica 'U. Dini', Università degli Studi di Firenze
viale Morgagni 67a, 50134 Firenze, Italy

Annalisa Buffa*

Institute of Mathematics, Ecole Polytechnique Fédérale de Lausanne
Station 8, 1015 Lausanne, Switzerland
Istituto di Matematica Applicata e Tecnologie Informatiche "E. Magenes" del CNR
via Ferrata 5, 27100 Pavia, Italy

Carlotta Giannelli

Dipartimento di Matematica e Informatica 'U. Dini', Università degli Studi di Firenze
viale Morgagni 67a, 50134 Firenze, Italy

Rafael Vázquez

Institute of Mathematics, Ecole Polytechnique Fédérale de Lausanne
Station 8, 1015 Lausanne, Switzerland
Istituto di Matematica Applicata e Tecnologie Informatiche "E. Magenes" del CNR
via Ferrata 5, 27100 Pavia, Italy

(Communicated by Siddhartha Mishra)

Abstract. We consider an adaptive isogeometric method (AIGM) based on (truncated) hierarchical B-splines and present the study of its numerical properties. By following [10, 12, 11], optimal convergence rates of the AIGM can be proved when suitable approximation classes are considered. This is in line with the theory of adaptive methods developed for finite elements, recently well reviewed in [43]. The important output of our analysis is the definition of classes of admissibility for meshes underlying hierarchical splines and the design of an optimal adaptive strategy based on these classes of meshes. The adaptivity analysis is validated on a selection of numerical tests. We also compare the results obtained with suitably graded meshes related to different classes of admissibility for 2D and 3D configurations.

1. **Introduction.** The design of efficient numerical schemes for the approximation of partial differential equations (PDEs) naturally demands suitable adaptive techniques, that automatically enable the refinement in well localized regions of the computational domain. The use of adaptive schemes is even more important in presence of singularities, when standard methods that do not support local mesh refinements do not achieve optimal convergence rates. In the context of isogeometric

---

analysis [27], the design and development of adaptive methods necessarily require suitable spline spaces with local refinement capabilities.

The hierarchical spline model is one of the most elegant solutions to easily define adaptive spline constructions, see e.g., [31, 49], and it has been successfully applied in challenging engineering applications [34, 46, 36]. In particular, truncated hierarchical B-splines (THB-splines) [24] properly meet the requirements needed for developing not only effective geometric modeling tools, but also efficient computational schemes [30, 23]. Indeed, THB-splines have been succesfully used in the design and analysis of adaptive techniques for elliptic problems in [10, 12, 11], on which this review is based upon, while analogous schemes for hierarchical splines have been studied in [20] or in [8] as well as in the very recent contributions [1, 41]. Adaptive techniques for boundary integro-differential equations have been introduced in [18, 19]. The main difference between the approach presented in this review and the ones presented in the papers cited above is that our refinement strategy is based on THB-splines, while other approaches are based on the standard hierarchical basis. For this reason, our adaptive strategy may produce less refined meshes for the same error thresholds [6].

Besides hierarchical splines, other types of splines have been successfully used to design adaptive isogeometric methods. For example, the first use of adaptivity in the context of isogeometric methods was based on T-splines [47, 2, 15], see also [17, 44], while their analysis suitable [35] or dual compatible [3, 4] formulations have been used to design refinement strategies with linear complexity, as in [40, 38]. Another example is the one of LR-splines, first defined in [14] and used in an adaptive setting in e.g., [28, 32, 33]. For a numerical comparison of all these approaches, we refer to [29, 26]. We remark that, unlike for hierarchical splines, the mathematical theory of adaptive methods based on T-splines or LR-splines has not been developed so far.

For our analysis, we consider the elliptic model problem:

$$- \operatorname{div}(\mathbf{A}\nabla u) = f \quad \text{in } \Omega, \qquad u\big|_{\partial\Omega} = 0, \tag{1}$$

where $\Omega \subset \mathbb{R}^d$, $d \geq 1$, is a bounded domain with Lipschitz boundary $\partial\Omega$, f is any square integrable function and the tensor $\mathbf{A}$ satisfies

$$\forall \mathbf{x} \in \Omega, \ \boldsymbol{\xi} \in \mathbb{R}^d \ \eta_1|\boldsymbol{\xi}|^2 \leq \mathbf{A}(x)\boldsymbol{\xi} \cdot \boldsymbol{\xi} \ \text{ and } \ |\mathbf{A}(\mathbf{x})\boldsymbol{\xi}| \leq \eta_2|\boldsymbol{\xi}|$$

with $0 < \eta_1 \leq \eta_2$. Analogously to adaptive finite elements, the solution of the model problem with an adaptive isogeometric method (AIGM) is obtained by an iterative procedure, where each iteration of the adaptivity loop consists of the following four key steps:

$$\boxed{\text{SOLVE}} \rightarrow \boxed{\text{ESTIMATE}} \rightarrow \boxed{\text{MARK}} \rightarrow \boxed{\text{REFINE}}.$$

Following the guidelines from the theory of adaptive finite elements, see e.g. [42, 43], the theory of convergence for adaptive isogeometric methods, using THB-splines with residual error estimators, has been recently developed in [10, 12, 11]. One of the key ingredients of the theoretical analysis is the definition of (strictly) admissible classes of hierarchical meshes. This class governs the maximum number of levels of THB-splines that do not vanish on any mesh element, and in practice it requires the mesh to be sufficiently graded.

In the present paper we review the convergence results developed in [10, 12, 11], considering and analyzing each of the four steps of the adaptive loop. We also

complement the previous works by studying the performance of the method in a selection of numerical tests.

The content of the next sections is as follows. Some preliminary aspects of hierarchical B-spline constructions are reviewed in Section 2 together with the definition of THB-splines and related properties, before introducing the notion of (strictly) admissible meshes. The module SOLVE and ESTIMATE of the adaptive isogeometric method are discussed in Sections 3 and 4, respectively. To define the module SOLVE and compute the numerical solution of problem (1), we consider the Galerkin method on hierarchical spline spaces in connection with admissible mesh configurations. An a posteriori error analysis in terms of both local upper and lower bound for the energy error is also presented. Section 5 deals with the MARK and REFINE modules. We first recall a well-known marking strategy, and then introduce a refinement strategy that preserves the class of admissibility during the adaptive loop. Section 6 is devoted to the result of optimal convergence, while Section 7 presents some numerical examples to analyze how the class of admissibility influences convergence. We end with some concluding remarks.

2. **Hierarchical splines and admissible meshes.** We consider a nested sequence of N tensor-product d-variate spline spaces $V^0 \subset V^1 \subset \ldots \subset V^{N-1}$ defined on a closed hyper-rectangle D in $\mathbb{R}^d$. Let $\widehat{\mathcal{B}}^\ell$ be the tensor-product B-spline basis of level ℓ, $\ell = 0, 1, \ldots, N-1$, and degree $\mathbf{p} = (p_1, \ldots, p_d)$, defined on the grid $\widehat{G}^\ell$. In each coordinate direction, the knot vectors at level zero are assumed to be open so that the first and the last knots are repeated $p_i + 1$ times, for $i = 1, \ldots, d$. B-splines are the standard form for spline representation in computer aided (geometric) design, see e.g., [13, 45]. They are locally linearly independent and non-negative. In addition they have local support and form a partition of unity. When nested spline spaces are considered, there exists a two-scale relation so that any function $s \in V^\ell \subset V^{\ell+1}$ can be expressed as

$$s = \sum_{\widehat{\beta} \in \widehat{\mathcal{B}}^{\ell+1}} c_{\widehat{\beta}}^{\ell+1}(s) \widehat{\beta}, \tag{2}$$

in terms of the coefficients $c_{\widehat{\beta}}^{\ell+1}$.

Let $\widehat{\Omega}^0 \supseteq \widehat{\Omega}^1 \supseteq \ldots \supseteq \widehat{\Omega}^{N-1}$ be a nested sequence of closed subsets of D, such that

$$\widehat{\Omega}^\ell = \bigcup_{\widehat{Q} \in \mathcal{R}^{\ell-1}} \overline{\widehat{Q}},$$

with $\mathcal{R}^{\ell-1} \subset \widehat{G}^{\ell-1}$ the refined elements of level $\ell - 1$. Let

$$\widehat{\mathcal{G}}^\ell := \left\{ \widehat{Q} \in \widehat{G}^\ell : \widehat{Q} \subset \widehat{\Omega}^\ell \wedge \widehat{Q} \not\subset \widehat{\Omega}^{\ell+1} \right\} \quad \text{and} \quad \widehat{\mathcal{Q}} := \left\{ \widehat{Q} \in \widehat{\mathcal{G}}^\ell, \ell = 0, \ldots, N-1 \right\} \tag{3}$$

be the collection of active (i.e., no more refined) elements at level ℓ and the hierarchical mesh, respectively. For any element $\widehat{Q}$ of the hierarchical mesh $\widehat{\mathcal{Q}}$, we assume that

$$h_{\widehat{Q}} \lesssim \text{diam}(\widehat{Q}) \lesssim h_{\widehat{Q}} \tag{4}$$

where $h_{\widehat{Q}} := |\widehat{Q}|^{1/d}$. Note that the symbol $\lesssim$ is used here and it what follows to denote an inequality which does not depend on the number of hierarchical levels. A mesh $\widehat{\mathcal{Q}}^*$ is a refinement of $\widehat{\mathcal{Q}}$, usually indicated as $\widehat{\mathcal{Q}}^* \succeq \widehat{\mathcal{Q}}$, if each element $\widehat{Q}^* \in \widehat{\mathcal{Q}}^*$ either also belongs to $\widehat{\mathcal{Q}}$ or is obtained by refinement of an element of $\widehat{\mathcal{Q}}$.
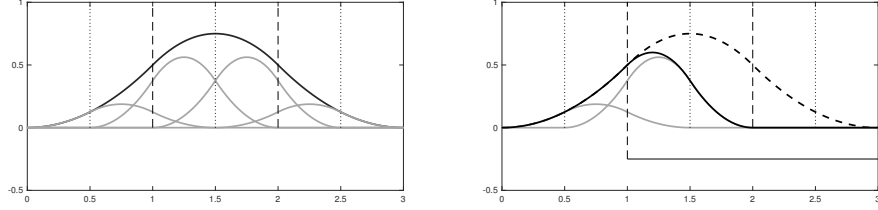
FIGURE 1. A univariate quadratic B-spline of level ℓ (left) and its truncation obtained by considering $\Omega^{\ell+1} = [1, 3.0]$ (right).

The hierarchical B-spline basis can be defined as follows, see also [31, 49].

Definition 1. The hierarchical B-spline (HB-spline) basis $\widehat{\mathcal{H}}$ with respect to the mesh $\widehat{\mathcal{Q}}$ is defined as

$$\widehat{\mathcal{H}}(\widehat{\mathcal{Q}}) := \left\{ \widehat{\beta} \in \widehat{\mathcal{B}}^\ell : \operatorname{supp} \widehat{\beta} \subseteq \widehat{\Omega}^\ell \wedge \operatorname{supp} \widehat{\beta} \nsubseteq \widehat{\Omega}^{\ell+1}, \ell = 0, \ldots, N - 1 \right\}.$$

Hierarchical B-splines are non-negative, linearly independent, and define nested hierarchical spline spaces, see e.g., [49]. The study of the hierarchical spline space was presented in [22] and [37] for the bivariate case with single knots and the general multivariate setting with arbitrary knot multiplicities, respectively. By considering suitable mesh configurations, it was there proved that span $\widehat{\mathcal{H}}(\widehat{\mathcal{Q}})$ contains all piecewise polynomial functions defined over the hierarchical mesh. From a practical point of view, uniform knot vectors and a fixed degree are usually considered at all levels, however the hierarchical B-spline model can be also applied with non-uniform mesh configurations and increasing degrees, as long as the tensor-product spaces in the sequence remain nested.

The following definition introduces the truncated basis for hierarchical splines [24] and hinges on the notion of the so-called *truncation*, namely

$$\operatorname{trunc}^{\ell+1} s := \sum_{\widehat{\beta} \in \widehat{\mathcal{B}}^{\ell+1}, \, \operatorname{supp} \widehat{\beta} \nsubseteq \widehat{\Omega}^{\ell+1}} c_{\widehat{\beta}}^{\ell+1}(s) \widehat{\beta}, \tag{5}$$

where $c_{\widehat{\beta}}^{\ell+1}(s)$ is the coefficient of the function $s \in V^\ell$ with respect to $\widehat{\beta}$ introduced in equation (2). By starting from the two-scale relation (2), the truncation of the function s with respect to level $\ell + 1$ defined by (5) considers only the B-splines of level $\ell + 1$ which do not belong to $\widehat{\mathcal{H}}(\widehat{\mathcal{Q}})$. Figure 1 shows an example of truncation for a univariate quadratic B-spline. When iteratively applied to hierarchical basis functions, the truncation eliminates from coarser B-splines the contribution of B-splines introduced at subsequent refinement levels, according to the following definition.

Definition 2. The truncated hierarchical B-spline (THB-spline) basis $\widehat{\mathcal{T}}$ with respect to the mesh $\widehat{\mathcal{Q}}$ is defined as

$$\widehat{\mathcal{T}}(\widehat{\mathcal{Q}}) := \left\{ \operatorname{Trunc}^{\ell+1} \widehat{\beta} : \widehat{\beta} \in \widehat{\mathcal{B}}^\ell \cap \widehat{\mathcal{H}}(\widehat{\mathcal{Q}}), \ell = 0, \ldots, N - 1 \right\},$$

where $\operatorname{Trunc}^{\ell+1} \widehat{\beta} := \operatorname{trunc}^{N-1}(\operatorname{trunc}^{N-2}(\ldots (\operatorname{trunc}^{\ell+1}(\widehat{\beta})) \ldots))$, for any $\widehat{\beta} \in \widehat{\mathcal{B}}^\ell \cap \widehat{\mathcal{H}}(\widehat{\mathcal{Q}})$.

The *level* of a THB-spline $\widehat{\tau} = \mathrm{Trunc}^{\ell+1}\,\widehat{\beta}$ in $\widehat{\mathcal{T}}(\widehat{\mathcal{Q}})$ is the level of its corresponding mother function $\widehat{\beta}$. We will denote $\widehat{\mathcal{H}} = \widehat{\mathcal{H}}(\widehat{\mathcal{Q}})$, $\widehat{\mathcal{T}} = \widehat{\mathcal{T}}(\widehat{\mathcal{Q}})$ when there will be no ambiguity in the text. THB-splines span the same space of HB-splines, are non-negative, linearly independent, and form a partition of unity [24]. In addition, they are a strongly stable basis, see [25] for the details. The two properties of non-negativity and partition of unity imply the convex hull property, which facilitates adaptive modeling operations [30]. Note that the reduced support of THB-splines with respect to HB-splines decreases the overlapping of basis functions introduced at different levels of the spline hierarchy.

In order to develop an adaptivity theory that exploits the reduced support of THB-splines with respect to standard hierarchical B-splines, the notion of *admissible meshes* was introduced in [7].

Definition 3. A mesh $\widehat{\mathcal{Q}}$ is admissible of class m if the truncated basis functions in $\widehat{\mathcal{T}}(\widehat{\mathcal{Q}})$ which take non-zero values over any element $\widehat{Q} \in \widehat{\mathcal{Q}}$ belong to at most m successive levels.

When an admissible mesh $\widehat{\mathcal{Q}}$ of class m is considered, the number of THB-splines in $\widehat{\mathcal{T}}(\widehat{\mathcal{Q}})$ which are non-zero on each mesh element is bounded. In particular, it is less than $m\prod_{i=1}^{d}(p_i+1)$. Moreover, if $\widehat{\mathcal{Q}}$ is an admissible mesh, any truncated basis function $\widehat{\tau} \in \widehat{\mathcal{T}}(\widehat{\mathcal{Q}})$ satisfies

$$|\widehat{Q}| \lesssim |\operatorname{supp}\widehat{\tau}| \lesssim |\widehat{Q}| \qquad \forall \widehat{Q} \in \widehat{\mathcal{Q}} \; : \; \widehat{Q} \cap \operatorname{supp}\widehat{\tau} \neq \emptyset.$$

Note that the hidden constants in the above inequalities depend on m but not on $\widehat{\tau}$, $\widehat{\mathcal{Q}}$ or N.

To easily link the local support of THB-splines to a certain subset of admissible meshes, we extend the definition of the *support extension* of a mesh element to the hierarchical setting as follows.

Definition 4. The support extension $S(\widehat{Q}, k)$ of an element $\widehat{Q} \in \widehat{G}^\ell$ with respect to level k, with $0 \leq k \leq \ell$, is defined as

$$S(\widehat{Q}, k) := \left\{ \widehat{Q}' \in \widehat{G}^k : \exists\, \widehat{\beta} \in \widehat{\mathcal{B}}^k,\, \operatorname{supp}\widehat{\beta} \cap \widehat{Q}' \neq \emptyset \wedge \operatorname{supp}\widehat{\beta} \cap \widehat{Q} \neq \emptyset \right\}.$$

To keep the notation as simple as possible, we will also denote by $S(\widehat{Q}, k)$ the region occupied by the closure of elements in $S(\widehat{Q}, k)$. By considering the auxiliary subdomains

$$\widehat{\omega}^\ell := \bigcup \left\{ \overline{\widehat{Q}} \; : \; \widehat{Q} \in \widehat{G}^\ell \wedge S(\widehat{Q}, \ell) \subseteq \widehat{\Omega}^\ell \right\},$$

for $\ell = 0, \ldots, N-1$, we arrive at the following proposition.

Proposition 5. *Let $\widehat{Q}$ be the mesh of active elements defined according to* (3) *with respect to the domain hierarchy $\widehat{\Omega}^0 \supseteq \widehat{\Omega}^1 \supseteq \ldots \supseteq \widehat{\Omega}^{N-1}$. If*

$$\widehat{\Omega}^\ell \subseteq \widehat{\omega}^{\ell-m+1},$$

for $\ell = m, m+1, \ldots, N-1$, then the mesh $\widehat{\mathcal{Q}}$ is admissible of class m.

The proof of this result can be found in [10]. As we will see in Section 5, it is possible to define refinement algorithms such that the constructed meshes satisfy the assumptions in the proposition. This relevant set of admissible meshes, called *strictly admissible meshes*, is defined as follows.

Definition 6. A mesh $\widehat{\mathcal{Q}}$ is strictly admissible of class m if it verifies the assumptions of Proposition 5.

The meshes considered in Section 7 are examples of strictly admissible meshes of different classes.

Remark 7. In [20] admissible meshes for hierarchical B-splines, instead of THB-splines, were considered by limiting the interaction between the basis functions acting on any mesh element to 2 consecutive values (analogous to consider $m = 2$ with respect to HB-splines in Definition 3). This kind of admissible refinements for $m \geq 2$ were also considered in [39]. A general framework for the design and implementation of (strictly) admissible refinements for HB- and THB-splines was recently presented in [6]. The properties of the hierarchical mesh configurations obtained with these algorithms were there analyzed and compared.

3. **The module SOLVE.** Let $\widehat{\mathcal{T}}_0$ be the truncated basis defined on an initial strictly admissible mesh $\widehat{\mathcal{Q}}_0$. We assume that the computational domain is defined as

$$\mathbf{x} \in \overline{\Omega}, \quad \mathbf{x} = \mathbf{F}(\widehat{\mathbf{x}}) = \sum_{\widehat{\tau} \in \widehat{\mathcal{T}}_0} \mathbf{C}_{\widehat{\tau}} \widehat{\tau}(\widehat{\mathbf{x}}), \qquad \widehat{\mathbf{x}} \in \widehat{\Omega}^0$$

with $\mathbf{C}_{\widehat{\tau}} \in \mathbb{R}^d$. We also assume that the mapping $\mathbf{F} : \widehat{\Omega}^0 \to \overline{\Omega}$ is a bi-Lipschitz homeomorphism:

$$\|D^\alpha \mathbf{F}\|_{L^\infty(\widehat{\Omega}^0)} \leq C_{\mathbf{F}}, \quad \|D^\alpha \mathbf{F}^{-1}\|_{L^\infty(\Omega)} \leq c_{\mathbf{F}}^{-1}, \qquad |\alpha| \leq 1, \tag{6}$$

where $c_{\mathbf{F}}$ and and $C_{\mathbf{F}}$ are independent constants bounded away from infinity.

To define the variational formulation of problem (1), we consider the space of functions in $H^1(\Omega)$ with vanishing trace on $\partial\Omega$

$$\mathbb{V} := H_0^1(\Omega) := \left\{ v \in H^1(\Omega) : v\big|_{\partial\Omega} = 0 \right\},$$

endowed with the norm $\|u\|_{\mathbb{V}}^2 = \|\nabla v\|_{L^2(\Omega)^d}^2 + \|v\|_{L^2(\Omega)}^2$. A weak solution of (1) is a function $u \in \mathbb{V}$ satisfying

$$u \in \mathbb{V} : \quad a(u, v) = \langle f, v \rangle, \quad \forall\, v \in \mathbb{V}, \tag{7}$$

where $a : \mathbb{V} \times \mathbb{V} \to \mathbb{R}$ is the bilinear form

$$a(u, v) := \int_\Omega \mathbf{A} \nabla u \cdot \nabla v, \qquad \forall\, u, v \in \mathbb{V},$$

and $f \in L^2(\Omega)$. Due to the assumptions on $\mathbf{A}$, the bilinear form $a(u, v)$ is coercive and continuous:

$$a(u, u) \geq \alpha_1 \|u\|_{\mathbb{V}}^2, \qquad a(u, v) \leq \alpha_2 \|u\|_{\mathbb{V}} \|v\|_{\mathbb{V}}, \qquad u, v \in \mathbb{V},$$

with constants α_1 and α_2, respectively. In addition, it induces the *energy norm* $|||v|||_\Omega := a(v, v)^{1/2}$, $\forall v \in \mathbb{V}$. The coercivity and continuity properties of $a(u, v)$ imply the equivalence between the energy and the $H^1(\Omega)$ norms on $\mathbb{V}$. The Lax-Milgram theorem ensures the existence and uniqueness of the weak solution (7).

All the notation introduced in the previous section for the parametric domain is now used in the computational domain by simply removing the $\widehat{\cdot}$. In particular, for any admissible mesh $\widehat{\mathcal{Q}} \succeq \widehat{\mathcal{Q}}_0$ and truncated basis $\widehat{\mathcal{T}}(\widehat{\mathcal{Q}})$, the corresponding mesh and functions of the physical domain are defined as

$$\tau(\mathbf{x}) = \widehat{\tau}(\widehat{\mathbf{x}}), \qquad \mathbf{x} = \mathbf{F}(\widehat{\mathbf{x}}).$$

The basis $\mathcal{T}(\mathcal{Q})$ collects the mapped THB-splines with respect to the hierarchical mesh $\mathcal{Q}$ on the domain Ω, and $\mathbb{S}(\mathcal{Q}) := \text{span}\,\mathcal{T}(\mathcal{Q})$. We denote by $\widehat{Q}$ the mesh element $Q = \mathbf{F}(\widehat{Q})$, and by $h_Q = |Q|^{1/d}$, where $|Q|$ represents the volume of Q, its size. In view of (4) and (6), we have: $h_Q \lesssim \text{diam}(Q) \lesssim h_Q$. We also set:

$$\Omega^\ell = \mathbf{F}(\widehat{\Omega}^\ell), \quad \omega^\ell = \mathbf{F}(\widehat{\omega}^\ell), \quad \mathcal{G}^\ell = \{Q \in \mathcal{Q} \,:\, \widehat{Q} \in \widehat{\mathcal{G}}^\ell\}, \quad G^\ell = \{Q \subset \Omega \,:\, \widehat{Q} \in \widehat{G}^\ell\}.$$

Analogously, the support extension of $Q \in \mathcal{G}^\ell$ with respect to level k is given by

$$S(Q, k) = \{Q' \in G^k \,:\, \widehat{Q}' \in S(\widehat{Q}, k)\}. \tag{8}$$

Finally, when $\mathcal{Q}^\star$ is a refinement of $\mathcal{Q}$, we will write $\mathcal{Q}^\star \succeq \mathcal{Q}$, when their pre-images $\widehat{\mathcal{Q}}^\star$ and $\widehat{\mathcal{Q}}$ satisfy $\widehat{\mathcal{Q}}^\star \succeq \widehat{\mathcal{Q}}$.

We define the module SOLVE of the AIGM as the Galerkin discretization of (7) in terms of hierarchical splines on Ω, that corresponds to

$$\text{find } U \in \mathbb{S}_D(\mathcal{Q}): \quad a(U, V) = \langle f, V \rangle, \quad \forall V \in \mathbb{S}_D(\mathcal{Q}), \tag{9}$$

where $\mathbb{S}_D(\mathcal{Q}) = \mathbb{S}(\mathcal{Q}) \cap H_0^1(\Omega)$. For simplicity, even if not strictly needed, we assume $\mathbb{S}_D(\mathcal{Q}) \subset C^1(\Omega)$. The general case could be treated on the line of the classical theory of adaptive finite element methods.

4. **The module ESTIMATE.** Let u be the exact weak solution of the model problem (7). The residual $\langle r, v \rangle := \langle f, v \rangle - a(U, v)$ associated to $U \in \mathbb{S}_D$ is the functional in the dual space to $\mathbb{V}$ that satisfies

$$\langle r, v \rangle = a(u - U, v), \quad \forall v \in \mathbb{V}, \qquad a(u - U, V) = \langle r, V \rangle = 0, \quad \forall V \in \mathbb{S}.$$

The module ESTIMATE of the AIGM computes the error indicator

$$\varepsilon_\mathcal{Q}^2(U, \mathcal{Q}) = \sum_{Q \in \mathcal{Q}} \varepsilon_\mathcal{Q}^2(U, Q) \qquad \text{with} \qquad \varepsilon_\mathcal{Q}^2(U, Q) = h_Q^2 \|r\|_{L^2(Q)}^2, \tag{10}$$

which is defined in terms of the element residual $r = f + \text{div}(\mathbf{A}\nabla U)$. Note that the residual does not contain any edge contribution as in a typical finite element setting, due to the assumption $\mathbb{S}_D(\Omega) \subset C^1(\Omega)$.

The a posteriori error analysis of the adaptive isogeometric methods was presented in [10] leading to the upper and lower bound for the Galerkin error:

$$\|u - U\|_\mathbb{V} \lesssim \varepsilon_\mathcal{Q}(U, \mathcal{Q}) \lesssim \|u - U\|_\mathbb{V} + \text{osc}_\mathcal{Q}(U, \mathcal{Q}), \tag{11}$$

where the oscillations are defined as

$$\text{osc}_\mathcal{Q}^2(U, \mathcal{Q}) = \sum_{Q \in \mathcal{Q}} \text{osc}^2(U, Q) \quad \text{with} \quad \text{osc}(U, Q) = h_Q \|r - \Pi_\mathbf{n} r\|_{L^2(Q)},$$

and $\Pi_\mathbf{n} : L^2(Q) \to \mathbb{Q}_\mathbf{n}$, $\mathbf{n} = (n_1, \ldots, n_d)$, denotes the L^2 projector onto the space of polynomials of degree n_j in the space direction j. Note that the hidden constants in (11) do not depend on the mesh size and the hierarchical level.

While (11) directly leads to a local version of the lower bound, namely

$$\varepsilon_\mathcal{Q}(U, Q) \lesssim \|u - U\|_{\mathbb{V}(Q)} + \text{osc}_\mathcal{Q}(U, Q),$$

a separate study is necessary to derive a *local upper bound*. Let $\mathcal{Q}$ and $\mathcal{Q}^*$ be two admissible meshes so that $\mathcal{Q}^* \succeq \mathcal{Q}$. The corresponding Galerkin solutions $U \in \mathbb{S}_D(\mathcal{Q})$ and $U^* \in \mathbb{S}_D(\mathcal{Q}^*)$ of problem (9) satisfy

$$|||U - U^*|||_\Omega^2 \lesssim \varepsilon_\mathcal{Q}^2(U, \mathcal{R}), \tag{12}$$

where $\mathcal{R} := \mathcal{R}_{Q \to \mathcal{Q}^*}$ is the refined set of elements, namely the elements of $\mathcal{Q}$ that do not belong to $\mathcal{Q}^*$, and $\Omega_\mathcal{R} := \bigcup \{\overline{Q} : Q \in \mathcal{R}\}$.

Remark 8. The local version of the upper bound in (12) was derived in [11] by exploiting a well selected quasi-interpolation operator $\mathcal{I}_{\mathcal{Q}}$ on hierarchical spline spaces that satisfies

$$\mathcal{I}_{\mathcal{Q}} w = w \quad \text{in} \quad \Omega_{\mathcal{Q}} := \Omega \setminus \Omega_{\mathcal{R}},$$

for $w \in \mathbb{S}_D(\mathcal{Q}^*)$. In order to do this, a class of L^2-stable quasi-interpolation operators onto the space of splines on tensor-product meshes [9] was suitably combined with hierarchical quasi-interpolants expressed in terms of the truncated basis [48].

5. **The modules MARK and REFINE.** The module MARK of the AIGM selects and marks a set of elements $\mathcal{M} \subset \mathcal{Q}$ according to Dörfler's marking [16]. A set of marked elements $\mathcal{M}$ such that

$$\varepsilon_{\mathcal{Q}}(U, \mathcal{M}) \geq \theta \, \varepsilon_{\mathcal{Q}}(U, \mathcal{Q}),$$

is suitably selected by considering a fixed parameter $\theta \in (0, 1]$. Even if for the convergence of method, the cardinality of this set is not crucial, it plays a key role for deriving the optimality of the method in Section 6. In particular, its minimal cardinality is required in Lemma 14 below where a suitable bound of the number of elements marked at the iterative step k is provided.

The REFINE module is based on a refinement strategy which exploits the properties of THB-splines for obtaining strictly admissible meshes between two successive steps of the adaptive loop. Note that the strict version of admissibility is considered in order to keep the refinement routine as simple as possible while still exploiting the effect of the truncation on the support of THB-splines. By recalling the definition of the support extension $S(Q, k)$ of an element Q with respect to level k introduced in (8), the refinement should be recursively propagated to a certain *neighborhood* of every marked element.

Definition 9. The neighborhood of $Q \in \mathcal{Q} \cap \mathcal{G}^\ell$ with respect to m is defined as

$$\mathcal{N}(\mathcal{Q}, Q, m) := \left\{ Q' \in \mathcal{G}^{\ell-m+1} : \exists \, Q'' \in S(Q, \ell-m+2), Q'' \subseteq Q' \right\},$$

when $\ell - m + 1 \geq 0$, and $\mathcal{N}(\mathcal{Q}, Q, m) = \emptyset$ for $\ell - m + 1 < 0$.

The automatic refinement of the AIGM is based on the definition of the RE-FINE and REFINE_RECURSIVE modules presented in Figure 2, that were first introduced in [10]. The fundamental properties of these algorithms, summarized in Lemma 10 and Proposition 11 below, were analyzed and proved in [10].
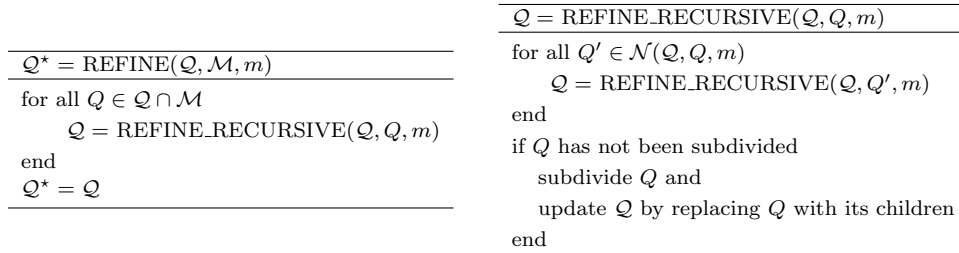
$\mathcal{Q}^\star = \text{REFINE}(\mathcal{Q}, \mathcal{M}, m)$
for all $Q \in \mathcal{Q} \cap \mathcal{M}$
$\mathcal{Q} = \text{REFINE\_RECURSIVE}(\mathcal{Q}, Q, m)$
end
$\mathcal{Q}^\star = \mathcal{Q}$

$\mathcal{Q} = \text{REFINE\_RECURSIVE}(\mathcal{Q}, Q, m)$
for all $Q' \in \mathcal{N}(\mathcal{Q}, Q, m)$
$\mathcal{Q} = \text{REFINE\_RECURSIVE}(\mathcal{Q}, Q', m)$
end
if Q has not been subdivided
subdivide Q and
update $\mathcal{Q}$ by replacing Q with its children
end

FIGURE 2. The REFINE and REFINE_RECURSIVE modules.

Lemma 10. *(Recursive refinement) Let $\mathcal{Q}$ be a strictly admissible mesh of class m. The call to $\mathcal{Q}^* = REFINE\_RECURSIVE(\mathcal{Q}, Q, m)$ terminates and returns a refined mesh $\mathcal{Q}^*$ with elements that either were already active in $\mathcal{Q}$ or are obtained by single refinement of an element of $\mathcal{Q}$.*

Proposition 11. *Let $\mathcal{Q}$ be a strictly admissible mesh of class $m \geq 2$ and let $Q_{\mathcal{M}}$ be an active element of level ℓ, for some $0 \leq \ell \leq N - 1$. The call to $\mathcal{Q}^* = REFINE\_RECURSIVE (\mathcal{Q}, Q_{\mathcal{M}}, m)$ returns a strictly admissible mesh $\mathcal{Q}^* \succeq \mathcal{Q}$ of class m.*

Proposition 11 is one of the most important results of our theory, since it guarantees that the strict class of admissibility of the mesh is preserved by the internal REFINE_RECURSIVE module. The same property naturally extends to the REFINE procedure.

Corollary 12. *Let $\mathcal{Q}$ be a strictly admissible mesh of class $m \geq 2$ and $\mathcal{M}$ the set of elements of $\mathcal{Q}$ marked for refinement. The call to $\mathcal{Q}^* = REFINE (\mathcal{Q}, \mathcal{M}, m)$ terminates and returns a strictly admissible mesh $\mathcal{Q}^* \succeq \mathcal{Q}$ of class m.*

The adaptivity analysis of hierarchical isogeometric methods also requires an estimate for the growth of the number of mesh elements with respect to the number of elements that are marked for refinement by the AIGM. Our estimate is in the line of the similar ones proved in the context of adaptive finite element methods. A linear complexity of this kind was derived in [12], by assuming the initial tensor-product grid as the image of open hypercubes with side length 1, and consequently $h_Q := 2^{-\ell}$ for all $Q \in G^\ell$. If $\mathcal{M} := \bigcup_{j=0}^{J-1} \mathcal{M}_j$ is the set of marked elements used to generate the sequence of strictly admissible meshes

$$\mathcal{Q}_j = \text{REFINE}(\mathcal{Q}_{j-1}, \mathcal{M}_{j-1}, m), \quad \mathcal{M}_{j-1} \subseteq \mathcal{Q}_{j-1} \quad \text{for } j \in \{1, \dots, J\},$$

there exists a constant $\Lambda > 0$ such that

$$\#\mathcal{Q}_J - \#\mathcal{Q}_0 \leq \Lambda \sum_{j=0}^{J-1} \#\mathcal{M}_j, \tag{13}$$

with $\Lambda = \Lambda(d, p, m) := 4(4\tilde{C} + 1)^d$, where $\tilde{C} := \left(2^{-1} + \frac{2}{1-2^{1-m}} C_s\right)$ and $C_s := 2^{m-2}(2\,p+1)$. Note, however, that this result can also be generalized to the current setting by suitably taking into account the corresponding maximum local mesh size.

A last remark concerning the hierarchical refinement should be devoted to the *overlay* mesh $\mathcal{Q}_* := \mathcal{Q}_1 \otimes \mathcal{Q}_2$ of two meshes $\mathcal{Q}_1, \mathcal{Q}_2$ obtained as the coarsest common refinement of $\mathcal{Q}_1$ and $\mathcal{Q}_2$. When strictly admissible meshes are considered, the overlay is still strictly admissible [12] and its cardinality satisfies [5, 40]

$$\#\mathcal{Q}_* = \#(\mathcal{Q}_1 \otimes \mathcal{Q}_2) \leq \#\mathcal{Q}_1 + \#\mathcal{Q}_2 - \#\mathcal{Q}_0, \tag{14}$$

where $\mathcal{Q}_0$ is the initial mesh configuration. Even if both the complexity estimate (13) and the overlay inequality (14) were obtained on the parametric domain $\widehat{\Omega}$ in [12], they also hold on physical meshes defined as images of parametric meshes.

6. **Optimal convergence.** Let $\mathbb{Q}^m$ be the set of strictly admissible refinements of class m obtained starting from $\mathcal{Q}_0$. Let $\mathbb{Q}_M^m \subset \mathbb{Q}^m$,

$$\mathbb{Q}_M^m := \{\mathcal{Q} \in \mathbb{Q}^m : \#\mathcal{Q} - \#\mathcal{Q}_0 \leq M\},$$

be the set of refinements of $\mathcal{Q}_0$ whose number of elements differs at most M by the one of $\mathcal{Q}_0$.

We define the *approximation class* $\mathbb{A}_s$ as

$$\mathbb{A}_s := \left\{ (v, f, \mathbf{A}) : |v, f, \mathbf{A}|_s := \sup_{M>0} \left(M^s \sigma(M; v, f, \mathbf{A}) \right) < \infty \right\},$$

for $s > 0$, where

$$\sigma(M; u, f, \mathbf{A}) := \inf_{\mathcal{Q} \in \mathbb{Q}_M^m} \sigma_e(\mathcal{Q}; u, f, \mathbf{A})^{1/2}$$

characterizes the quality of the best approximation in $\mathbb{Q}_M^m$ with respect to the *best total error* defined as

$$\sigma_e(\mathcal{Q}; u, f, \mathbf{A}) := \inf_{V \in \mathbb{S}_D(\mathcal{Q})} \left(|||u - V|||_\Omega^2 + \mathrm{osc}_\mathcal{Q}^2(V, \mathcal{Q}) \right).$$

A complete analysis of these approximation classes is still missing and goes beyond the scope of this paper. In particular, the connection and possible dependence of the class of approximation on the value of m have not been identified.

In the paper [11], the following two additional results associated to the considered AIGM were recently given.

Lemma 13. *(Quasi-optimality of total error) Let $\mathcal{Q} \in \mathbb{Q}^m$ be a strictly admissible mesh. The total error associated to the Galerkin solution $U \in \mathbb{S}_D(\mathcal{Q})$ of problem (9) on $\mathbb{S}_D(\mathcal{Q})$ satisfies*

$$|||u - U|||_\Omega^2 + \mathrm{osc}_\mathcal{Q}^2(U, \mathcal{Q}) \lesssim \inf_{V \in \mathbb{S}_D(\mathcal{Q})} \left(|||u - V|||_\Omega^2 + \mathrm{osc}_\mathcal{Q}^2(V, \mathcal{Q}) \right).$$

Lemma 14. *(Cardinality of $\mathcal{M}_k$) Assume that the module MARK selects a set $\mathcal{M}_k$ of marked elements with minimal cardinality, and the marking parameter θ to be small enough. Let u be the solution of the model problem (1). If $(u, f, \mathbf{A}) \in \mathbb{A}_s$, the AIGM generates a sequence $\{\mathcal{Q}_k, \mathbb{S}_D(\mathcal{Q}_k), U_k\}_{k \geq 0}$ of strictly admissible meshes, hierarchical spline spaces, and discrete solutions so that*

$$\#\mathcal{M}_k \lesssim |u, f, \mathbf{A}|_s^{1/s} \left[|||u - U_k|||_\Omega^2 + \mathrm{osc}_{\mathcal{Q}_k}^2(U_k, \mathcal{Q}_k) \right]^{-\frac{1}{2s}},$$

for any $k \geq 0$.

The quasi-optimality result, summarized in the next theorem, was also proved in [11] by exploiting Lemmas 13 and 14, together with the complexity estimate (13), the (global) lower bound in (11), and the contraction property [10].

Theorem 15. *Let the marking parameter θ satisfy $\theta \in (0, \theta_*)$ with θ_* small enough, and assume that the module MARK selects a set $\mathcal{M}_k$ of marked elements with minimal cardinality. Let u be the solution of the model problem (1). If $(u, f, \mathbf{A}) \in \mathbb{A}_s$, the AIGM generates a sequence $\{\mathcal{Q}_k, \mathbb{S}_D(\mathcal{Q}_k), U_k\}_{k \geq 0}$ of strictly admissible meshes, hierarchical spline spaces, and discrete solutions so that*

$$\left[|||u - U_k|||_\Omega^2 + \mathrm{osc}_{\mathcal{Q}_k}^2(U_k, \mathcal{Q}_k) \right]^{\frac{1}{2}} \lesssim |u, f, \mathbf{A}|_s (\#\mathcal{Q}_k - \#\mathcal{Q}_0)^{-s},$$

for any $k \geq 1$.

7. **Numerical examples.** In this section we show the performance of the adaptive isogeometric method by applying it to Poisson problem

$$\begin{cases} -\Delta u = f & \text{in } \Omega, \\ u = g_D & \text{on } \Gamma_D, \\ \dfrac{\partial u}{\partial n} = g_N & \text{on } \Gamma_N, \end{cases}$$

where $\Gamma_D \cup \Gamma_N = \partial\Omega$, $\Gamma_D \cap \Gamma_N = \emptyset$ and $\Gamma_D \neq \emptyset$. We note that, to deal with Neumann boundary conditions, the error indicator must be modified in the following way

$$\epsilon_{\mathcal{Q}}^2(U,Q) = h_Q^2 \|r\|_{L^2(Q)}^2 + h_Q \|r_N\|_{L^2(\partial Q \cap \Gamma_N)}^2$$

where r is defined as in (10), and $r_N = \partial U / \partial n - g_N$. Although Neumann and non-homogeneous Dirichlet conditions are not covered by our theory, we have included such conditions in some of the numerical tests, since their main purpose is to analyze the behavior of the adaptive method when considering different degrees and different values of the admissibility class m. All the results are obtained by using the isogeometric Matlab/Octave GeoPDEs library, see [21].

We consider three different numerical tests with different kind of solutions: the first one with smooth solution, and the other two with singular solution, for which local refinement is required to obtain optimal convergence rates. For all the numerical tests, we discretize with hierarchical B-splines of degrees $\mathbf{p} = (p, p) = (2, 2), (3, 3), (4, 4)$ and we consider the admissibility classes $m = 2, 3, 4, \infty$, where $m = \infty$ corresponds to strictly consider the set of marked elements without refining any elements in the neighborhood in the REFINE_RECURSIVE module. The adaptivity algorithm is stopped when the hierarchical mesh reaches a certain number of levels (seven in the first example, nine in the second and eight in the third). At each step $k \geq 0$ of the adaptive procedure, for the approximate solution U_k in the hierarchical space $\mathbb{S}(\mathcal{Q}_k)$, we compute the error estimator $\varepsilon_{\mathcal{Q}_k}(U_k, \mathcal{Q}_k)$ and, when an exact solution is available, the H^1-seminorm of the error and the *effectivity index* I_e^k, defined as

$$I_e^k := \frac{\varepsilon_{\mathcal{Q}_k}(U_k, \mathcal{Q}_k)}{|u - U_k|_{H^1(\Omega)}}, \qquad k \geq 0.$$

Example 1: Smooth function with a peak. In the first numerical example the domain is the unit square $\Omega = (0, 1)^2$, and we impose Dirichlet boundary conditions on $\Gamma_D = \partial\Omega$, and a source function f such that the exact solution is given by

$$u(x, y) = e^{-100((x-0.5)^2 + (y-0.5)^2)},$$

which is shown on the left of Figure 3. The solution is a smooth function with a peak in the center of the domain.

For the adaptive algorithm the first iteration is computed in a Cartesian mesh of 4×4 elements, and Dörfler's marking strategy is performed setting the parameter $\theta = 0.25$. On the left of Figure 4 we show the behavior of the error and of the estimator during adaptive refinement. With any of the considered values of degree p and admissibility class m we obtain the optimal convergence rate $O(N_d^{-p/2})$, where $N_d = \#\mathcal{T}(\mathcal{Q})$ is the number of degrees of freedom. Notice that since the solution is smooth, optimal convergence rate is also obtained with uniform refinement, but the adaptive method always requires less degrees of freedom.

On the right of Figure 4 we plot the effectivity index divided by 10. The effectivity index remains bounded from above and from below for all the values of the admissibility class, which indicates the good behavior of the estimator in all cases.

Although the convergence rates are optimal for all cases, independently of the admissibility class, there is a relative impact of the value of m in the number of refined elements, and consequently in the number of degrees of freedom. As expected, when the value of m is increased the refinement is more localized in the center of the domain, see Figure 5. This loss of locality for low values of m is also observed in the error plot of Figure 4, as the curve for m equal 2 remains slightly above those
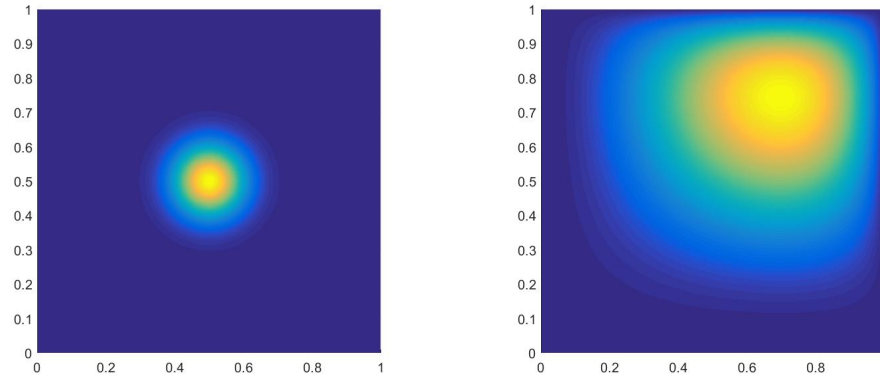
FIGURE 3. Exact solutions for the smooth function with a peak (left) and the singular function (right).

for m equal to 3 and 4. We also report, in Table 1, the total number of elements and degrees of freedom at the last iteration.

	$\mathbf{p} = (2,2)$		$\mathbf{p} = (3,3)$		$\mathbf{p} = (4,4)$	
	$\#\mathcal{Q}$	$\#\mathcal{T}(\mathcal{Q})$	$\#\mathcal{Q}$	$\#\mathcal{T}(\mathcal{Q})$	$\#\mathcal{Q}$	$\#\mathcal{T}(\mathcal{Q})$
$m = 2$	3232	2876	3880	3313	3736	3400
$m = 3$	2500	2244	3868	3317	2824	2224
$m = 4$	3628	3272	3064	2614	2224	1672
$m = \infty$	3616	3244	2980	2446	2284	1756

TABLE 1. Number of elements ($\#\mathcal{Q}$) and degrees of freedom ($\#\mathcal{T}(\mathcal{Q})$) for Example 1.

Example 2: Singular function. For the second numerical test, the domain is again the unit square $\Omega = (0,1)^2$, and we impose homogeneous Dirichlet boundary conditions on $\Gamma_D = \partial\Omega$, and a source function f such that the exact solution is given by

$$u(x,y) = x^{2.3}(1-x)y^{2.9}(1-y),$$

which is shown on the right of Figure 3. The adaptive algorithm is run with the same parameters of the previous example. In this case the solution belongs to $H^s(\Omega)$, for some $2 < s < 3$, with two different singularities on the edges $x = 0$ and $y = 0$. Hence, uniform refinement will not attain optimal convergence rates for high degree p, and local refinement near the two edges is necessary. This expected behavior is indeed observed in the convergence errors of Figure 6 (left). Moreover, the optimal convergence rate for adaptive refinement is obtained for all the values of the admissibility class m, with a slight improvement in terms of the number of degrees of freedom for higher m, as in the previous example.

On the right of Figure 6 we show the effectivity index divided by 10. As in the previous numerical test, the effectivity index remains bounded from above and from below for any degree and any value of m, which indicates that the estimator works properly both for smooth and singular solutions.

(a) Error and estimator, $\mathbf{p} = (2,2)$

(b) Effectivity index, $\mathbf{p} = (2,2)$

(c) Error and estimator, $\mathbf{p} = (3,3)$

(d) Effectivity index, $\mathbf{p} = (3,3)$

(e) Error and estimator, $\mathbf{p} = (4,4)$

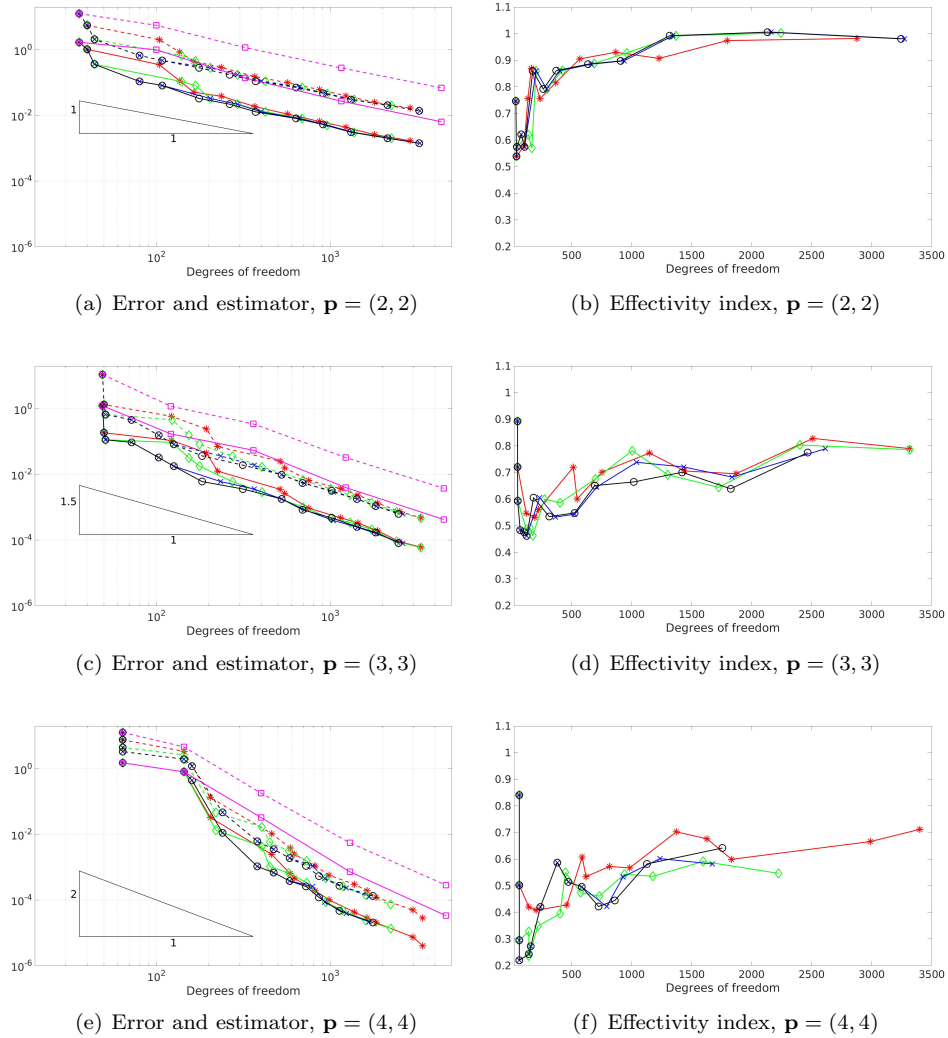(f) Effectivity index, $\mathbf{p} = (4,4)$

FIGURE 4. Numerical error and estimator (left) and effectivity index (right) for the smooth function with a peak. On the left, the error (solid lines) and the estimator (dashed lines) are plotted for different degrees. The red, green, blue and black lines (star, diamond, cross and circle markers, respectively) represent admissibility classes $m = 2, 3, 4, \infty$, respectively, while the magenta line (square marker) corresponds to uniform refinement. The same coloring and marking is used for the effectivity index (divided by 10) on the right figure.

We report in Table 2 the number of elements and degrees of freedom obtained at the last iteration of the adaptivity procedure. As expected, much coarser meshes can be used for high degree. This can be also verified from the plots of the hierarchical meshes in Figure 7. Moreover, increasing the value of m also reduces the number of elements, since refinement is less spread by the REFINE procedure.
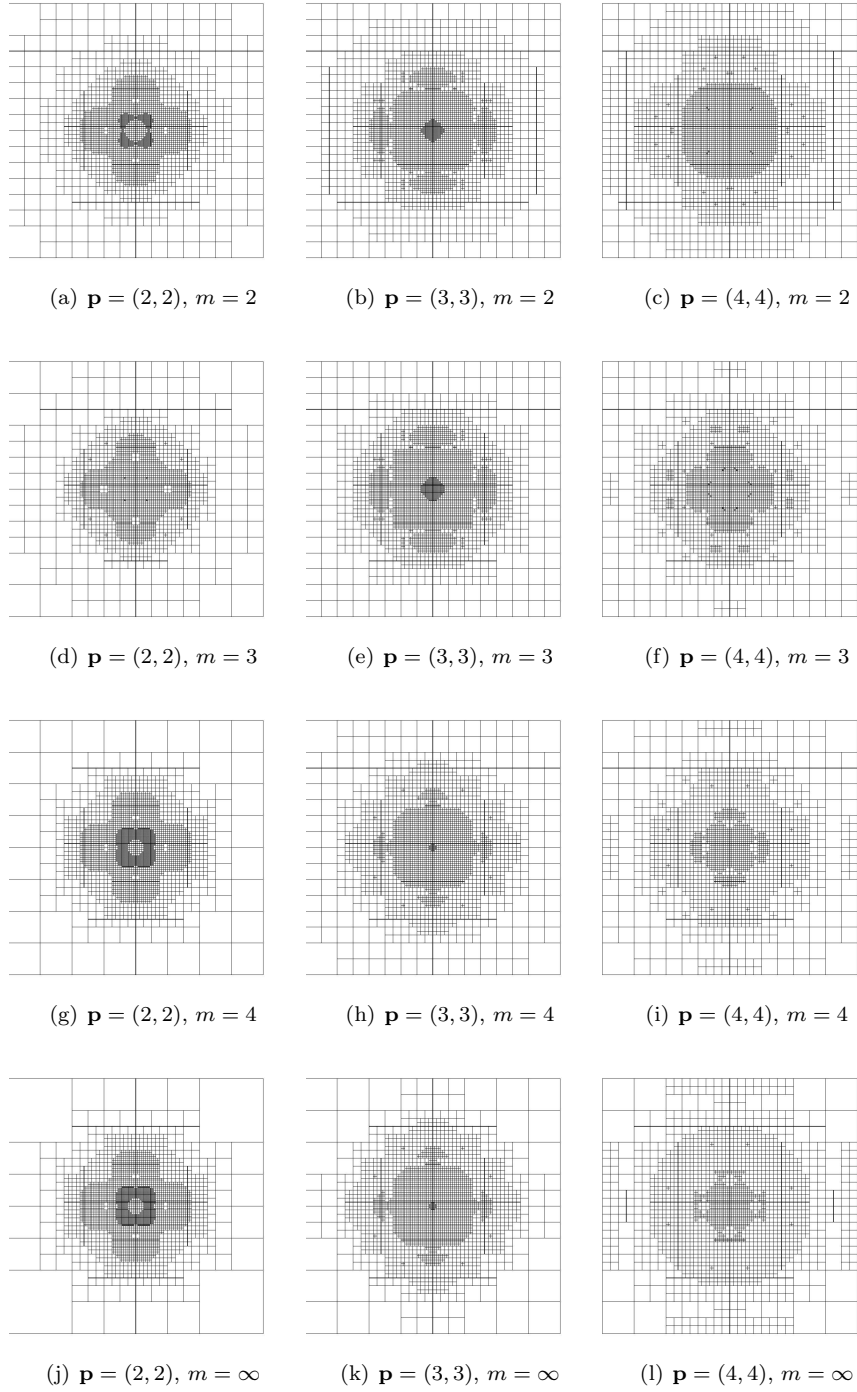
(a) $\mathbf{p} = (2, 2)$, $m = 2$ (b) $\mathbf{p} = (3, 3)$, $m = 2$ (c) $\mathbf{p} = (4, 4)$, $m = 2$

(d) $\mathbf{p} = (2, 2)$, $m = 3$ (e) $\mathbf{p} = (3, 3)$, $m = 3$ (f) $\mathbf{p} = (4, 4)$, $m = 3$

(g) $\mathbf{p} = (2, 2)$, $m = 4$ (h) $\mathbf{p} = (3, 3)$, $m = 4$ (i) $\mathbf{p} = (4, 4)$, $m = 4$

(j) $\mathbf{p} = (2, 2)$, $m = \infty$ (k) $\mathbf{p} = (3, 3)$, $m = \infty$ (l) $\mathbf{p} = (4, 4)$, $m = \infty$

FIGURE 5. Hierarchical meshes obtained for the smooth solution with a peak.

(a) Error and estimator, $\mathbf{p} = (2,2)$

(b) Effectivity index, $\mathbf{p} = (2,2)$

(c) Error and estimator, $\mathbf{p} = (3,3)$

(d) Effectivity index, $\mathbf{p} = (3,3)$

(e) Error and estimator, $\mathbf{p} = (4,4)$

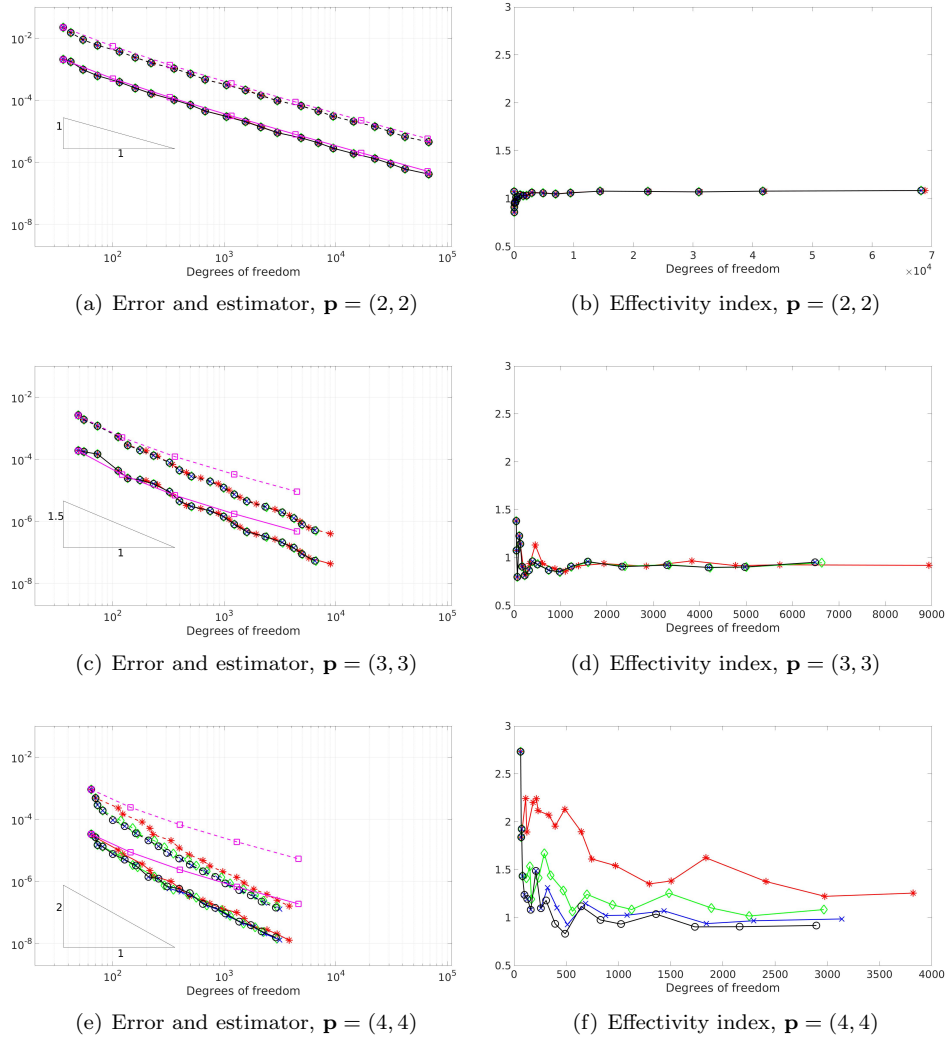(f) Effectivity index, $\mathbf{p} = (4,4)$

FIGURE 6. Numerical error and estimator (left) and effectivity index (right) for the example with singular solution. On the left, the error (solid lines) and the estimator (dashed lines) are plotted for different degrees. The red, green, blue and black lines (star, diamond, cross and circle markers, respectively) represent admissibility classes $m = 2, 3, 4, \infty$, respectively, while the magenta line (square marker) corresponds to uniform refinement. The same coloring and marking is used for the effectivity index (divided by 10) on the right figure.

In both examples any value of m provides the optimal convergence rate. In order to maximize the efficiency of the adaptive method, and to keep the number of degrees of freedom as small as possible, the numerical tests suggest that higher values of m should be used. We remark that in these examples optimal convergence

	$\mathbf{p} = (2,2)$		$\mathbf{p} = (3,3)$		$\mathbf{p} = (4,4)$	
	$\#\mathcal{Q}$	$\#\mathcal{T}(\mathcal{Q})$	$\#\mathcal{Q}$	$\#\mathcal{T}(\mathcal{Q})$	$\#\mathcal{Q}$	$\#\mathcal{T}(\mathcal{Q})$
$m = 2$	68677	68860	8776	8938	3700	3822
$m = 3$	68014	68201	6346	6631	2875	2966
$m = 4$	68008	68195	6208	6484	3010	3138
$m = \infty$	68008	68195	6208	6484	2827	2895

TABLE 2. Number of elements ($\#\mathcal{Q}$) and degrees of freedom ($\#\mathcal{T}(\mathcal{Q})$) for Example 2.

is also obtained for $m = \infty$, but it is important to note that this is not guaranteed by the theory.

Example 3: 3D example. For the last example we consider a three dimensional domain with non-trivial geometry. The domain is obtained by linear interpolation of two surfaces, where the first one is a quarter of a ring with inner and outer radius equal to one and two, respectively, while the second one is the same surface rotated 90 degrees around the z axis, and then translated by the vector $(0.5, 0, 1)$ (see Figure 8(a)). We consider a null source function, and impose a Neumann condition on the upper boundary with $g_N = 1$, and homogeneous Dirichlet conditions elsewhere. This generates singularities on the edges of the upper boundary. In this case the exact solution is not known, but an approximation is shown in Figure 8(b). For the adaptive algorithm we start with a mesh formed by one single element, and refine using Dörfler's marking strategy with a parameter $\theta = 0.75$. Since the exact solution is not known, we only present in Figure 9 the convergence of the error indicator. The adaptive method attains optimal convergence rates in terms of the degrees of freedom, which is now $O(N_d^{-p/3})$. Moreover, as in the previous examples better convergence is obtained with higher values of the admissibility class m, and this good behavior is even more evident in the current three-dimensional example than in the previous ones. Finally, we show in Figure 10 the restriction to the boundary of the final hierarchical mesh, for degree $\mathbf{p} = (4,4)$ and for all the chosen admissibility classes. The adaptive method localizes the refinement near the edges where the singularity is more pronounced. As in the two-dimensional examples, a lower value of m reduces the locality of the refinement, which propagates to the interior.

8. **Closure.** This paper is largely inspired by [11, 10, 12] and provides a comprehensive analysis of adaptive isogeometric methods based on truncated hierarchical B-splines with a residual-based error estimator. As it is natural, at each adaptive step, in order to restore the good properties of the mesh, i.e. to maintain its class of admissibility, refinement is done "around" marked elements. Although the complexity estimates derived in [12] prove that this procedure still enjoys optimal complexity, in practice we add a non-negligible number of degrees of freedom, and the question whether this is really needed remains open. Our numerical results give some insight about this problem: the larger m is chosen the less the proliferation of degrees of freedom is obtained while preserving optimal convergence rates. Additional numerical investigations on the best values of m and on the impact of such a proliferation on the computational cost for a given tolerance are object of ongoing research.
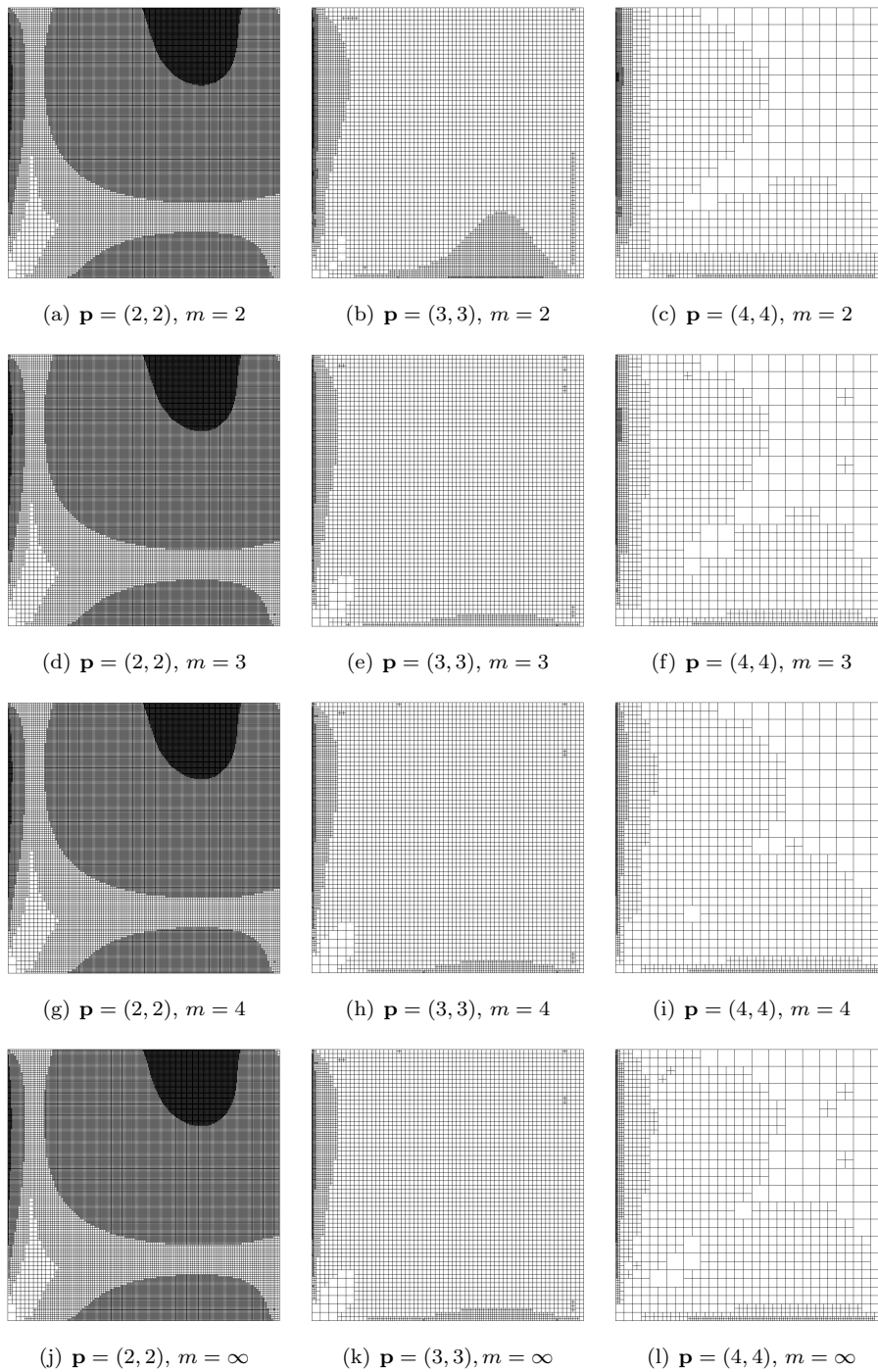
(a) $\mathbf{p} = (2, 2)$, $m = 2$ (b) $\mathbf{p} = (3, 3)$, $m = 2$ (c) $\mathbf{p} = (4, 4)$, $m = 2$

(d) $\mathbf{p} = (2, 2)$, $m = 3$ (e) $\mathbf{p} = (3, 3)$, $m = 3$ (f) $\mathbf{p} = (4, 4)$, $m = 3$

(g) $\mathbf{p} = (2, 2)$, $m = 4$ (h) $\mathbf{p} = (3, 3)$, $m = 4$ (i) $\mathbf{p} = (4, 4)$, $m = 4$

(j) $\mathbf{p} = (2, 2)$, $m = \infty$ (k) $\mathbf{p} = (3, 3)$, $m = \infty$ (l) $\mathbf{p} = (4, 4)$, $m = \infty$

FIGURE 7. Hierarchical meshes obtained for the example with singular solution.

(a) Geometry of the 3D example.

(b) Solution restricted to the boundary.
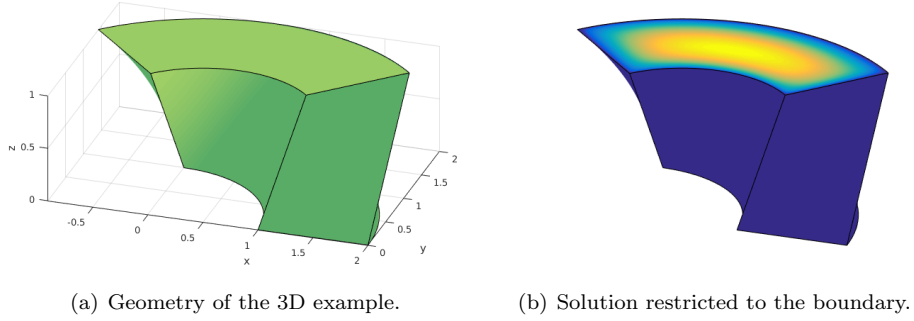
FIGURE 8. Geometry and solution for the 3D example.

(a) Estimator for $\mathbf{p} = (2, 2)$

(b) Estimator for $\mathbf{p} = (3, 3)$
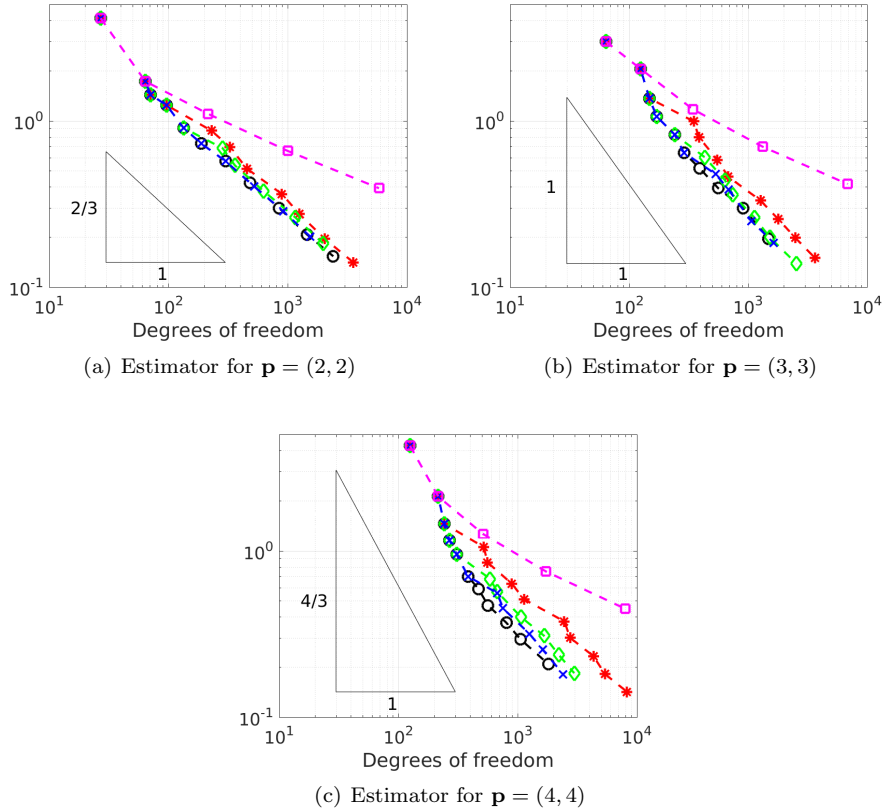
(c) Estimator for $\mathbf{p} = (4, 4)$

FIGURE 9. Convergence of the estimator for the 3D example. The red, green, blue and black lines (star, diamond, cross and circle markers, respectively) represent admissibility classes $m = 2, 3, 4, \infty$, respectively, while the magenta line (square marker) corresponds to uniform refinement.

(a) Mesh for $m = 2$ (b) Mesh for $m = 3$

(c) Mesh for $m = 4$ (d) Mesh for $m = \infty$
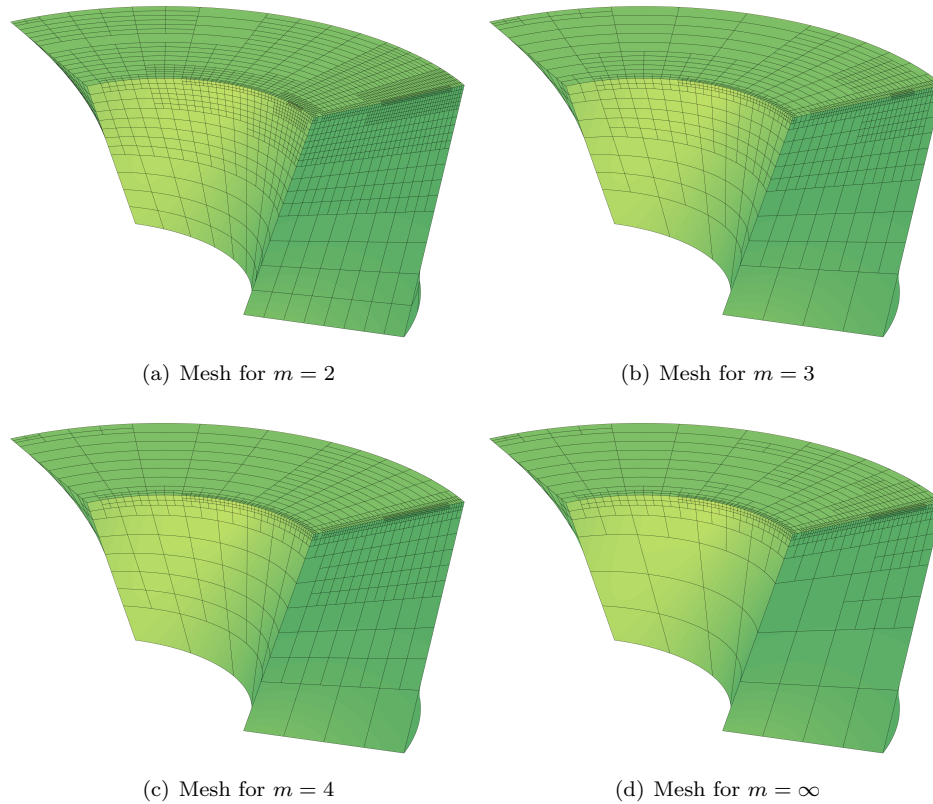
FIGURE 10. Meshes obtained for the 3D example degree $\mathbf{p} = (4, 4)$ and different values of the admissibility class m.

REFERENCES

[1] M. Actis, P. Morin and M. S. Pauletti, A new perspective on hierarchical spline spaces for adaptivity, arXiv:1808.02053

[2] Y. Bazilevs, V. M. Calo, J. A. Cottrell, J. Evans, T. J. R. Hughes, S. Lipton, M. A. Scott and T. W. Sederberg, Isogeometric analysis using T-Splines, *Comput. Methods Appl. Mech. Engrg.*, **199** (2010), 229–263.

[3] L. Beirão da Veiga, A. Buffa, D. Cho and G. Sangalli, Analysis-Suitable T-splines are Dual-Compatible, *Comput. Methods Appl. Mech. Engrg.*, **249/252** (2012), 42–51.

[4] L. Beirão da Veiga, A. Buffa, G. Sangalli and R. Vázquez, Analysis-suitable T-splines of arbitrary degree: Definition, linear independence and approximation properties, *Math. Models Methods Appl. Sci.*, **23** (2013), 1979–2003.

[5] A. Bonito and R. H. Nochetto, Quasi-optimal convergence rate of an adaptive discontinuous Galerkin method, *SIAM J. Numer. Anal.*, **48** (2010), 734–771.

[6] C. Bracco, C. Giannelli and R. Vázquez, Refinement algorithms for adaptive isogeometric methods with hierarchical splines, *Axioms*, **7** (2018), 43.

[7] A. Buffa and E. M. Garau, Refinable spaces and local approximation estimates for hierarchical splines, *IMA J. Numer. Anal.*, **37** (2017), 1125–1149.

[8] A. Buffa and E. M. Garau, A posteriori error estimators for hierarchical B-spline discretizations, *Math. Models Methods Appl. Sci.*, **28** (2018), 1453–1480.

[9] A. Buffa, E. M. Garau, C. Giannelli and G. Sangalli, On quasi-interpolation operators in spline spaces, in *Building Bridges: Connections and Challenges in Modern Approaches to Numerical Partial Differential Equations* (eds. G. R. Barrenechea et al.), vol. 114, Lecture Notes in Computational Science and Engineering, 2016, 73–91.

[10] A. Buffa and C. Giannelli, Adaptive isogeometric methods with hierarchical splines: Error estimator and convergence, *Math. Models Methods Appl. Sci.*, **26** (2016), 1–25.

[11] A. Buffa and C. Giannelli, Adaptive isogeometric methods with hierarchical splines: Optimality and convergence rates, *Math. Models Methods Appl. Sci.*, **27** (2017), 2781–2802.

[12] A. Buffa, C. Giannelli, P. Morgenstern and D. Peterseim, Complexity of hierarchical refinement for a class of admissible mesh configurations, *Comput. Aided Geom. Design*, **47** (2016), 83–92.

[13] C. de Boor, *A Practical Guide to Splines*, Springer, revised ed., 2001.

[14] T. Dokken, T. Lyche and K. F. Pettersen, Polynomial splines over locally refined box–partitions, *Comput. Aided Geom. Design*, **30** (2013), 331–356.

[15] M. R. Dörfel, B. Jüttler and B. Simeon, Adaptive isogeometric analysis by local h-refinement with T-splines, *Comput. Methods Appl. Mech. Engrg.*, **199** (2010), 264–275.

[16] W. Dörfler, A convergent adaptive algorithm for Poisson's equation, *SIAM J. Numer. Anal.*, **33** (1996), 1106–1124.

[17] E. J. Evans, M. A. Scott, X. Li and D. C. Thomas, Hierarchical T-splines: Analysis-suitability, Bézier extraction, and application as an adaptive basis for isogeometric analysis, *Comput. Methods Appl. Mech. Engrg.*, **284** (2015), 1–20.

[18] M. Feischl, G. Gantner, A. Haberl and D. Praetorius, Adaptive 2D IGA boundary element methods, *Engineering Analysis with Boundary Elements*, **62** (2016), 141–153.

[19] M. Feischl, G. Gantner, A. Haberl and D. Praetorius, Optimal convergence for adaptive IGA boundary element methods for weakly-singular integral equations, *Numer. Math.*, **136** (2017), 147–182.

[20] G. Gantner, D. Haberlik and D. Praetorius, Adaptive IGAFEM with optimal convergence rates: Hierarchical B-splines, *Math. Models Methods Appl. Sci.*, **27** (2017), 2631–2674.

[21] E. Garau and R. Vázquez, Algorithms for the implementation of adaptive isogeometric methods using hierarchical B-splines, *Appl. Numer. Math.*, **123** (2018), 58–87.

[22] C. Giannelli and B. Jüttler, Bases and dimensions of bivariate hierarchical tensor–product splines, *J. Comput. Appl. Math.*, **239** (2013), 162–178.

[23] C. Giannelli, B. Jüttler, S. K. Kleiss, A. Mantzaflaris, B. Simeon and J. Špeh, THB-splines: An effective mathematical technology for adaptive refinement in geometric design and isogeometric analysis, *Comput. Methods Appl. Mech. Engrg.*, **299** (2016), 337–365.

[24] C. Giannelli, B. Jüttler and H. Speleers, THB–splines: The truncated basis for hierarchical splines, *Comput. Aided Geom. Design*, **29** (2012), 485–498.

[25] C. Giannelli, B. Jüttler and H. Speleers, Strongly stable bases for adaptively refined multilevel spline spaces, *Adv. Comput. Math.*, **40** (2014), 459–490.

[26] P. Hennig, M. Kästner, P. Morgenstern and D. Peterseim, Adaptive mesh refinement strategies in isogeometric analysis— A computational comparison, *Comput. Methods Appl. Mech. Engrg.*, **316** (2017), 424–448.

[27] T. J. R. Hughes, J. A. Cottrell and Y. Bazilevs, Isogeometric analysis: CAD, finite elements, NURBS, exact geometry and mesh refinement, *Comput. Methods Appl. Mech. Engrg.*, **194** (2005), 4135–4195.

[28] K. A. Johannessen, T. Kvamsdal and T. Dokken, Isogeometric analysis using LR B-splines, *Comput. Methods Appl. Mech. Engrg.*, **269** (2014), 471–514.

[29] K. A. Johannessen, F. Remonato and T. Kvamsdal, On the similarities and differences between Classical Hierarchical, Truncated Hierarchical and LR B-splines, *Comput. Methods Appl. Mech. Engrg.*, **291** (2015), 64–101.

[30] G. Kiss, C. Giannelli, U. Zore, B. Jüttler, D. Großmann and J. Barner, Adaptive CAD model (re-)construction with THB–splines, *Graphical models*, **76** (2014), 273–288.

[31] R. Kraft, Adaptive and linearly independent multilevel B–splines, in *Surface Fitting and Multiresolution Methods* (eds. A. Le Méhauté, C. Rabut and L. L. Schumaker), Vanderbilt University Press, Nashville, 1997, 209–218.

[32] M. Kumar, T. Kvamsdal and K. A. Johannessen, Simple a posteriori error estimators in adaptive isogeometric analysis, *Comput. Math. Appl.*, **70** (2015), 1555–1582.

[33] M. Kumar, T. Kvamsdal and K. A. Johannessen, Superconvergent patch recovery and a posteriori error estimation technique in adaptive isogeometric analysis, *Comput. Methods Appl. Mech. Engrg.*, **316** (2017), 1086–1156.

[34] G. Kuru, C. V. Verhoosel, K. G. van der Zeeb and E. H. van Brummelen, Goal-adaptive isogeometric analysis with hierarchical splines, *Comput. Methods Appl. Mech. Engrg.*, **270** (2014), 270–292.

[35] X. Li, J. Zheng, T. W. Sederberg, T. J. R. Hughes and M. A. Scott, On linear independence of T-spline blending functions, *Comput. Aided Geom. Design*, **29** (2012), 63–76.

[36] G. Lorenzo, M. A. Scott, K. Tew, T. J. R. Hughes and H. Gomez, Hierarchically refined and coarsened splines for moving interface problems, with particular application to phase-field models of prostate tumor growth, *Comput. Methods Appl. Mech. Engrg.*, **319** (2017), 515–548.

[37] D. Mokriš, B. Jüttler and C. Giannelli, On the completeness of hierarchical tensor-product B-splines, *J. Comput. Appl. Math.*, **271** (2014), 53–70.

[38] P. Morgenstern, Globally structured three-dimensional analysis-suitable T-splines: definition, linear independence and m-graded local refinement, *SIAM J. Numer. Anal.*, **54** (2016), 2163–2186.

[39] P. Morgenstern, *Mesh Refinement Strategies for the Adaptive Isogeometric Method*, PhD thesis, Institut für Numerische Simulation, Rheinische Friedrich-Wilhelms-Universität Bonn, 2017.

[40] P. Morgenstern and D. Peterseim, Analysis-suitable adaptive T-mesh refinement with linear complexity, *Comput. Aided Geom. Design*, **34** (2015), 50–66.

[41] P. Morin, R. H. Nochetto and M. S. Pauletti, An adaptive method for hierarchical splines. A posteriori estimation via local problems, convergence and optimality, In preparation.

[42] R. H. Nochetto, K. G. Siebert and A. Veeser, Theory of adaptive finite element methods: An introduction, in *Multiscale, Nonlinear and Adaptive Approximation* (eds. R. DeVore and A. Kunoth), Springer Berlin Heidelberg, 2009, 409–542.

[43] R. H. Nochetto and A. Veeser, Primer of adaptive finite element methods, in *Multiscale and Adaptivity: Modeling, Numerics and Applications*, vol. 2040 of Lecture Notes in Math., Springer, Heidelberg, 2012, 125–225.

[44] D. Schillinger, L. Dedé, M. Scott, J. Evans, M. Borden, E. Rank and T. Hughes, An isogeometric design-through-analysis methodology based on adaptive hierarchical refinement of NURBS, immersed boundary methods, and T-spline CAD surfaces, *Comput. Methods Appl. Mech. Engrg.*, **249/252** (2012), 116–150.

[45] L. L. Schumaker, *Spline Functions: Basic Theory, 3rd Edition*, Cambridge University Press, 2007.

[46] M. A. Scott, D. C. Thomas and E. J. Evans, Isogeometric spline forests, *Comput. Methods Appl. Mech. Engrg.*, **269** (2014), 222–264.

[47] T. W. Sederberg, D. L. Cardon, G. T. Finnigan, N. S. North, J. Zheng and T. Lyche, T-spline simplification and local refinement, *ACM Trans. Graphics*, **23** (2004), 276–283.

[48] H. Speleers and C. Manni, Effortless quasi-interpolation in hierarchical spaces, *Numer. Math.*, **132** (2016), 155–184.

[49] A.-V. Vuong, C. Giannelli, B. Jüttler and B. Simeon, A hierarchical approach to adaptive local refinement in isogeometric analysis, *Comput. Methods Appl. Mech. Engrg.*, **200** (2011), 3554–3567.

E-mail address: cesare.bracco@unifi.it
E-mail address: annalisa.buffa@epfl.ch
E-mail address: carlotta.giannelli@unifi.it
E-mail address: rafael.vazquez@epfl.ch